Anomalous parity asymmetry of WMAP 7-year power spectrum data at low multipoles: Is it cosmological or systematics?

Jaiseung Kim* and Pavel Naselsky

Niels Bohr Institute and Discovery Center, Blegdamsvej 17, DK-2100 Copenhagen, Denmark

(Received 14 June 2010; published 1 September 2010)

It is natural to assume a parity-neutral Universe and accordingly no particular parity preference in the cosmic microwave background sky. However, our investigation based on the WMAP 7-year power spectrum shows there exists a large-scale odd-parity preference with high statistical significance. We also find that the odd-parity preference in WMAP7 data is slightly higher than earlier releases. We have investigated possible origins, and ruled out various noncosmological origins. We also find that the primordial origin requires $|\mathrm{Re}[\Phi(\mathbf{k})]| \ll |\mathrm{Im}[\Phi(\mathbf{k})]|$ for $k \lesssim 22/\eta_0$, where η_0 is the present conformal time. In other words, it requires translational invariance in the primordial Universe to be violated on scales larger than 4 Gpc. The Planck surveyor, which possesses wide frequency coverage and systematics distinct from the WMAP, may allow us to resolve the mystery of the anomalous odd-parity preference. Furthermore, polarization maps of large-sky coverage will reduce degeneracy in cosmological origins.

DOI: 10.1103/PhysRevD.82.063002 PACS numbers: 95.85.Sz, 98.70.Vc, 98.80.Cq, 98.80.Es

I. INTRODUCTION

In the past, there have been great successes in measurement of cosmic microwave background (CMB) anisotropy by ground and satellite observations [1–11]. CMB anisotropy, which is associated with the inhomogeneity of the last scattering surface, provides the deepest survey so far and allows us to constrain cosmological models significantly. Since the initial release of WMAP data, the WMAP CMB sky data have undergone scrutiny, and various anomalies have been found and reported [12–34]. In particular, CMB anisotropy at low multipoles is associated with scales far beyond any existing astrophysical survey, and therefore CMB anomalies at low multipoles may hint new physical laws at unexplored large scales.

The CMB sky map may be considered as the sum of even- and odd-parity functions. Previously, Land *et al.* have noted the odd point-parity preference of WMAP CMB data, but found its statistical significance is not high enough [24]. In our previous work, we have applied a slightly different estimator to WMAP 5-year power spectrum data, and found significant odd point-parity preference at low multipoles [33]. In this paper, we investigate the recently released WMAP 7-year data up to higher multipoles, and discuss origins of the observed odd-parity preference.

This paper is organized as follows. In Sec. II, we discuss the anomalous odd-parity preference of the WMAP data. In Sec. III, we implement cosmological fitting by excluding even or odd low multipole data. In Secs. IV and V, we investigate noncosmological and cosmological origin. In Sec. VI, we summarize our investigation and discuss prospects. In Appendix , we briefly review statistical properties of Gaussian CMB anisotropy.

*jkim@nbi.dk

II. PARITY ASYMMETRY OF THE WMAP DATA

The CMB anisotropy sky map may be considered as the sum of even- and odd-parity functions:

$$T(\hat{\mathbf{n}}) = T^+(\hat{\mathbf{n}}) + T^-(\hat{\mathbf{n}}), \tag{1}$$

where

$$T^+(\hat{\mathbf{n}}) = \frac{T(\hat{\mathbf{n}}) + T(-\hat{\mathbf{n}})}{2}, \tag{2}$$

$$T^-(\hat{\mathbf{n}}) = \frac{T(\hat{\mathbf{n}}) - T(-\hat{\mathbf{n}})}{2}. \tag{3}$$

Taking into account the parity property of spherical harmonics $Y_{\mathrm{lm}}(\hat{\mathbf{n}}) = (-1)^l Y_{\mathrm{lm}}(-\hat{\mathbf{n}})$ [35], we may easily show

$$T^+(\hat{\mathbf{n}}) = \sum_{l=2n,m} a_{\mathrm{lm}} Y_{\mathrm{lm}}(\hat{\mathbf{n}}), \tag{4}$$

$$T^-(\hat{\mathbf{n}}) = \sum_{l=2n-1,m} a_{\mathrm{lm}} Y_{\mathrm{lm}}(\hat{\mathbf{n}}), \tag{5}$$

where n is an integer. Therefore, significant power asymmetry between even and odd multipoles indicates a preference for a particular parity. Hereafter, we will denote a preference for a particular parity by ''parity asymmetry.'' In Fig. 1, we show the WMAP 7-year, 5-year, and 3-year data and the WMAP concordance model [1,4,36–38]. We may see from Fig. 1 that the power spectrum of WMAP data at even multipoles tends to be lower than those at neighboring odd multipoles. In Fig. 2, we show $(-1)^l l(l+1)/2\pi(C_l^{\mathrm{WMAP}} - C_l^{\Lambda\mathrm{CDM}})$ for low multipoles. Since we expect random scattering of data points around a theoretical model, we expect the distribution of dots in Fig. 2 to be

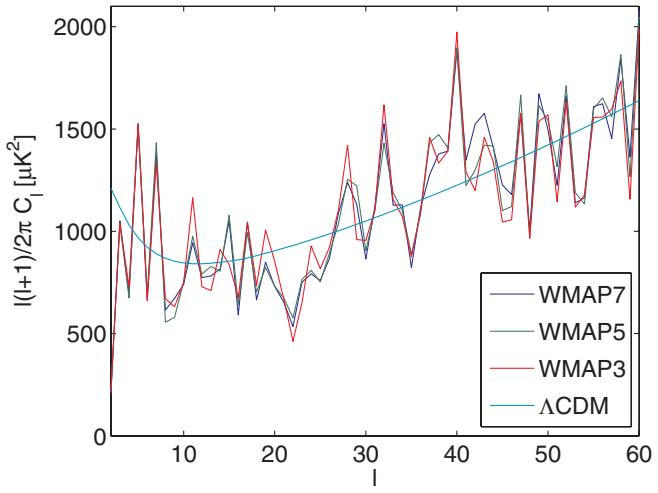

FIG. 1 (color online). CMB power spectrum: WMAP 7-year data (blue), WMAP 5-year data (green), and WMAP 3-year data (red), ΛCDM model (cyan).

symmetric around zero. However, there are only 5 points of positive values among 22 points in the case of WMAP7 or WMAP5 data. Therefore, we may see that there is the tendency of power deficit (excess) at even (odd) multipoles, compared with the ΛCDM model. Taking into account $l(l+1)C_l \sim$ const, we may consider the following quantities:

$$P^+ = \sum_{l=2}^{l_{\max}} 2^{-1}(1+(-1)^l) l(l+1)/2\pi C_l, \qquad (6)$$

$$P^- = \sum_{l=2}^{l_{\max}} 2^{-1}(1-(-1)^l) l(l+1)/2\pi C_l, \qquad (7)$$

where P^+ and P^- are the sum of $l(l+1)/2\pi C_l$ for even

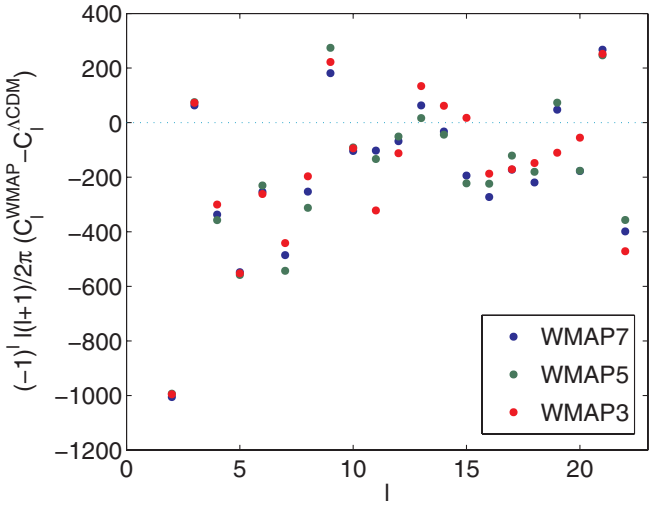

FIG. 2 (color online). $(-1)^l\times$ difference between WMAP power spectrum data and the ΛCDM model.

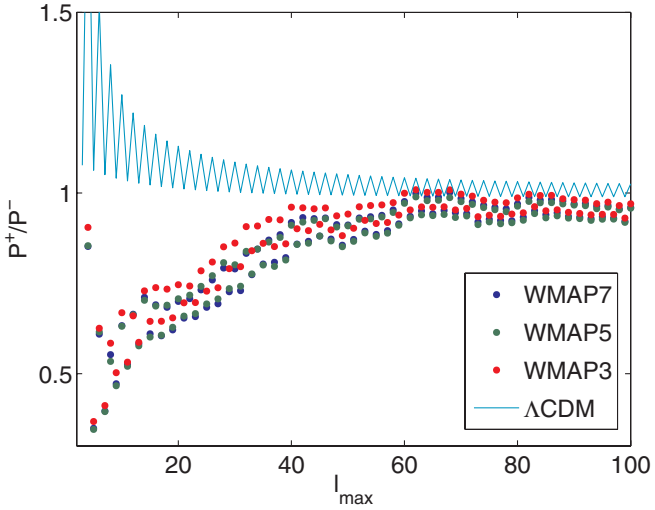

FIG. 3 (color online). P^+/P^- of WMAP data and ΛCDM.

and odd multipoles, respectively. Therefore, the ratio P^+/P^- is associated with the degree of the parity asymmetry, where the lower value of P^+/P^- indicates odd-parity preference, and vice versa. It is worth noting that our estimator of the parity asymmetry does not possess explicit dependence on the underlying theoretical model in the sense that the term $C_l^{\rm WMAP} - C_l^{\Lambda\rm CDM}$ is absent in our estimator.

In Fig. 3, we show the P^+/P^- of WMAP data, and a ΛCDM model for various $l_{\max}$. As shown in Fig. 3, P^+/P^- of WMAP data is far below theoretical values. Though the discrepancy is largest at lowest $l_{\max}$, its statistical significance is not necessarily high for low l, due to large statistical fluctuation. In order to make rigorous assessment on its statistical significance at low l, we are going to compare P^+/P^- of WMAP data with simulation. We have produced 10^4 simulated CMB maps HEALPIX Nside $= 8$ and Nside $= 512$, respectively, via map synthesis, with $a_{\rm lm}$ randomly drawn from Gaussian ΛCDM model. We have degraded the WMAP processing mask (Nside $= 16$) to Nside $= 8$, and set pixels to zero, if any of their daughter pixels is zero. After applying the mask, we have estimated power spectrum $2 \le l \le 23$ from simulated cut-sky maps (Nside $= 8$) by a pixel-based maximum likelihood method [1,39,40]. At the same time, we have applied the WMAP team's foreground KQ85 mask to the simulated maps (Nside $= 512$), and estimated power spectrum $2 \le l \le 1024$ by a pseudo-C_l method [41,42]. In the simulation, we have neglected instrument noise, since the signal-to-noise ratio of the WMAP data is quite high at multipoles of interest (i.e., $l \le 100$) [1,2]. Using the low l estimation by pixel-maximum likelihood method and high l estimation by pseudo-C_l method, we have computed P^+/P^-, respectively, for various multipole ranges $2 \le l \le l_{\max}$, and compared P^+/P^- of the WMAP data with simulation. In Fig. 4, we show the p-value of WMAP7, WMAP5, and WMAP3, respectively, for various $l_{\max}$, where p-value

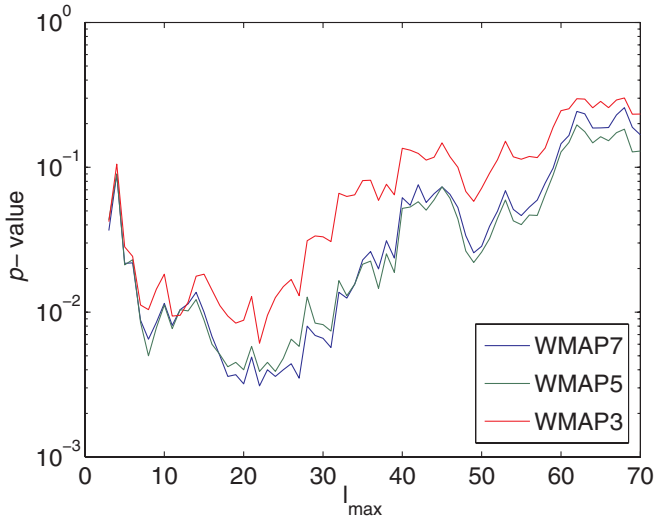

FIG. 4 (color online). Probability of getting P^+/P^- as low as WMAP data for multipole range $2 \leq l \leq l_{\max}$.

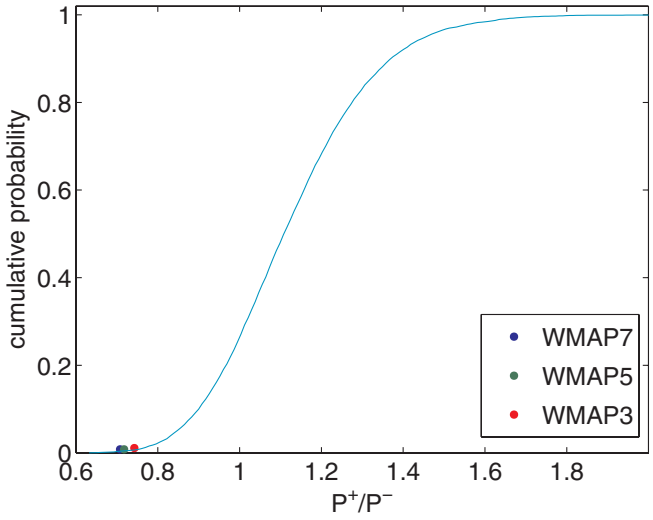

FIG. 5 (color online). Parity asymmetry at multipoles ($2 \leq l \leq 22$): cumulative distribution of P^+/P^- for 10^4 simulated maps (cyan), P^+/P^- of WMAP7 (blue), WMAP5 (green), and WMAP3 (red).

denotes fractions of simulations as low as P^+/P^- of the WMAP data. As shown in Fig. 4, the parity asymmetry of WMAP7 data at multipoles ($2 \leq l \leq 22$) is most anomalous, where the p-value is 0.0031. As shown in Fig. 4, the statistical significance of the parity asymmetry (i.e., low p-value) is getting higher, when we include higher multipoles up to 22. Therefore, we may not attribute the odd-parity preference simply to the low quadrupole power, and find it rather likely that the low quadrupole power is not an isolated anomaly, but shares an origin with the odd-parity preference.

In Table I, we summarize P^+/P^- and p-values of WMAP7, WMAP5, and WMAP3 for $l_{\max} = 22$. As shown in Fig. 4 and Table I, the odd-parity preference of WMAP7 is most anomalous, while WMAP7 data are believed to have more accurate calibration and less foreground contamination than earlier releases. [1–4,43]. In Fig. 5, we show cumulative distribution of P^+/P^- for 10^4 simulated maps. The values corresponding to P^+/P^- of WMAP data are marked as dots. We have also compared P^+/P^- of the WMAP7 with whole-sky simulation (i.e., no mask), and obtained a p-value of 0.002 for $l_{\max} = 22$. The lower p-value from whole-sky simulation is attributed to the fact that statistical fluctuation in whole-sky C_l estimation is smaller than that of cut-sky estimation.

In the absence of strong theoretical grounds for the parity asymmetry ($2 \leq l \leq 22$), we have to take into account our *posteriori* choice on $l_{\max}$, which might have enhanced the statistical significance. In order to do that, we have produced whole-sky Monte-Carlo simulations and retained only simulations whose p-value is lowest at $l_{\max} = 22$. The p-values have been estimated by comparing them with simulations, which are produced separately. Once we retained 10^4 simulations, we compared them with WMAP7 data, and found that only a fraction (0.0197) of retained simulations have P^+/P^- as low as WMAP7 data. The statistical significance of the parity asymmetry ($2 \leq l \leq 22$) is reduced substantially by accounting for the *posteriori* choice on $l_{\max}$. However, it is still significant.

We have also investigated the parity asymmetry with respect to mirror reflection (i.e., $l + m =$ even or odd respectively) in galactic coordinates and ecliptic coordinates. However, we find the statistical significance is not as high as the point-parity asymmetry (i.e., $l =$ even or odd).

TABLE I. The parity asymmetry of WMAP data ($2 \leq l \leq 22$).

Data	P^+/P^-	p-value
WMAP7	0.7076	0.0031
WMAP5	0.7174	0.0039
WMAP3	0.7426	0.0061

III. THE POWER CONTRAST AND THE ΛCDM MODEL FITTING

The parity asymmetry discussed in the previous section is explicitly associated with the angular power spectrum data, which are used extensively to fit cosmological models. Noting the significant power contrast between even and odd low multipoles, we have investigated cosmological models, respectively, by excluding even or odd low multipole data ($2 \leq l \leq 22$) from the total data set. Hereafter, we denote CMB data of even (odd) multipoles ($2 \leq l \leq 22$) plus all high multipoles as D_2 (D_3), respectively. For a cosmological model, we have considered ΛCDM + SZ effect + weak lensing, where SZ is the Sunayev-Zeldovich effect and cosmological parameters are $\lambda \in \{\Omega_b, \Omega_c, \tau, n_s, A_s, A_{sz}, H_0\}$. For data constraints, we have used the WMAP 7-year power spectrum data [1]. In order

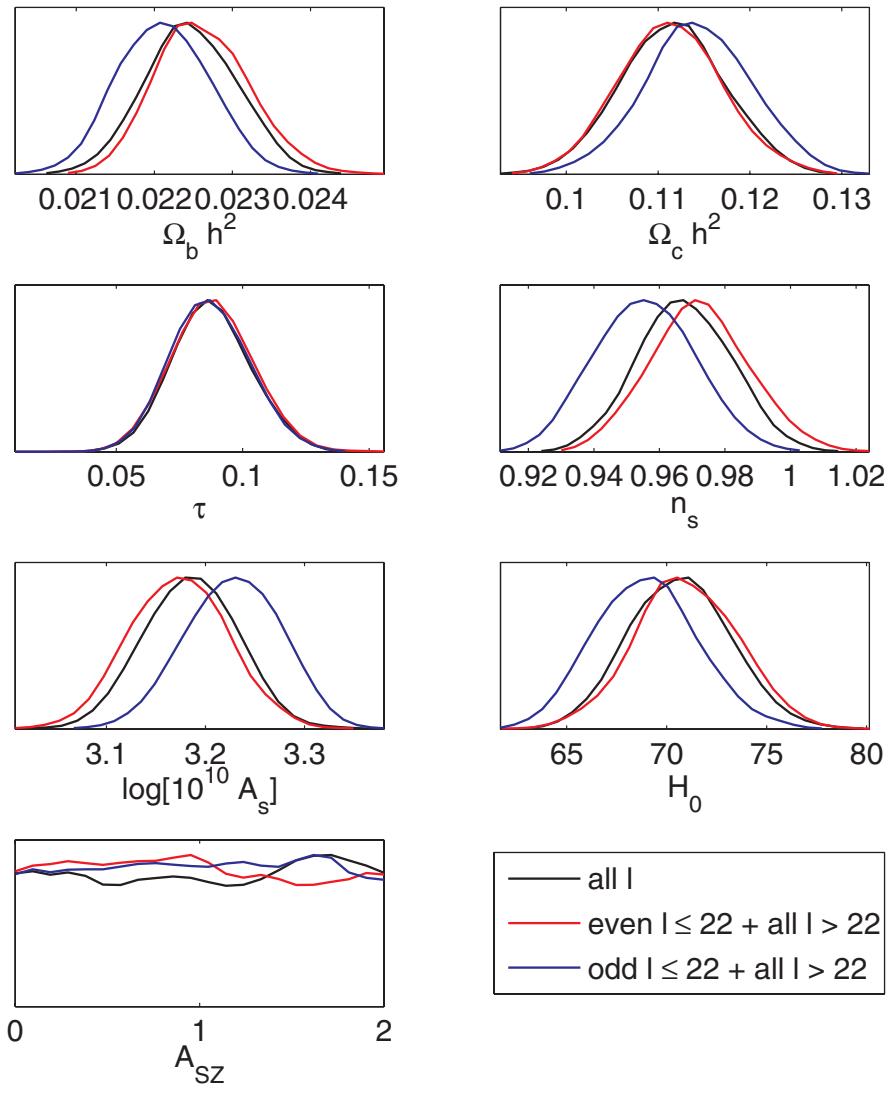

FIG. 6 (color online). Marginalized likelihood of cosmological parameters: results are obtained, respectively, with or without even or odd multipole data ($2 \leq l \leq 22$).

to exclude even or odd low multipoles, we have made slight modifications to the likelihood code provided by the WMAP team, and run COSMOMC with the modification. [1,44–46]. In Fig. 6, we show the marginalized likelihoods of parameters. As shown in Fig. 6, the parameter likelihood imposed by D_3 seems to differ from those of others. In Table II, we show the best-fit parameters and 1σ confidence intervals, where λ, λ_2, and λ_3 denote the best-fit values of the full data, D_2 and D_3, respectively. As mentioned above, there exists some level of tension

TABLE II. Cosmological parameters (ΛCDM + SZ + lens).

	λ	λ_2	λ_3
$\Omega_b h^2$	0.0226 ± 0.0006	0.0228 ± 0.0006	0.0221 ± 0.0006
$\Omega_c h^2$	0.112 ± 0.006	0.11 ± 0.006	0.116 ± 0.006
τ	0.0837 ± 0.0147	0.0879 ± 0.015	0.087 ± 0.0147
n_s	0.964 ± 0.014	0.974 ± 0.015	0.95 ± 0.015
$\log[10^{10} A_s]$	3.185 ± 0.047	3.165 ± 0.049	3.246 ± 0.048
H_0	70.53 ± 2.48	71.43 ± 2.51	68.07 ± 2.53
A_{sz}	$1.891^{+0.109}_{-1.891}$	$1.469^{+0.541}_{-1.469}$	$1.558^{+0.442}_{-1.558}$

between D_3 and the full data. However, the Bayes factor $\mathcal{L}(\lambda|D_3)/\mathcal{L}(\lambda_3|D_3) = \exp(-3733.124 + 3732.791) = 0.71$ shows that it is "not worth more than a bare mention," according to Jeffreys' scale [47].

IV. NONCOSMOLOGICAL ORIGINS

In this section, we are going to investigate noncosmological origins such as asymmetric beams, instrument noise, foreground, and the cut-sky effect.

A. Asymmetric beam

The shape of the WMAP beams are slightly asymmetric [43,48,49], while the WMAP team has assumed symmetric beams in the power spectrum estimation [1,4,43,48]. We have investigated the association of beam asymmetry with the anomaly, by relying on simulated maps provided by [49]. The authors have produced 10 simulated maps for each frequency and differencing assembly (D/A) channels, where the detailed shape of the WMAP beams and the WMAP scanning strategy are taken into account [49]. From simulated maps, we have estimated P^+ and P^-, where we have compensated for beam smoothing purposely by the WMAP team's beam transfer function (i.e., symmetric beams). In Fig. 7, we show P^+ and P^- values of the simulated maps, and the dashed lines of a slope corresponding to P^+/P^- of ΛCDM and WMAP7 data, respectively. As shown in Fig. 7, we do not observe the odd-parity preference of WMAP data in simulated maps. Therefore, we find it hard to attribute the odd-parity preference to asymmetric beams.

B. Noise

There exists instrument noise in the WMAP data. Especially, $1/f$ noise, when coupled with WMAP scanning pattern, may result in less accurate measurement at certain low multipoles [36,50,51]. In order to investigate the association of noise with the anomaly, we have produced

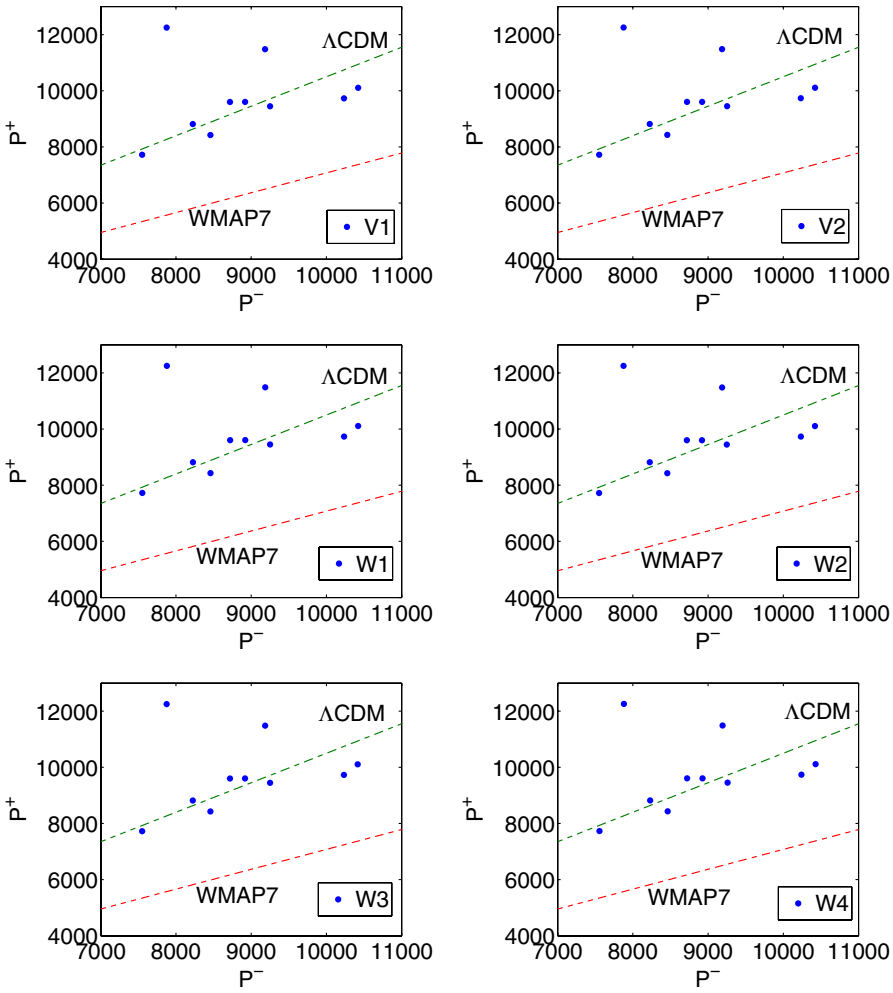

FIG. 7 (color online). Parity asymmetry in the presence of beam asymmetry: dots denote (P^+, P^-) of CMB maps simulated with asymmetric beams. The dashed lines are plotted with slopes corresponding to the P^+/P^- of the ΛCDM model (red) and WMAP7 data (green), respectively. The alphanumeric values at the lower right corner denote the frequency band and D/A channel.

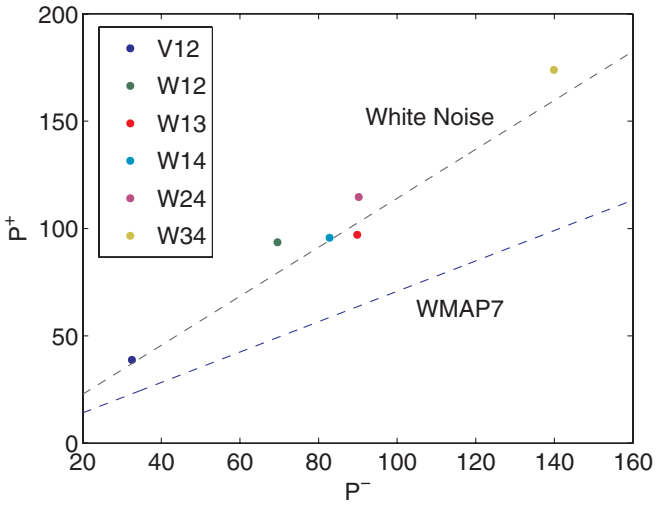

FIG. 8 (color online). Parity asymmetry of the WMAP noise: dots denote (P^+, P^-) of noise maps, and alphanumeric values in the legend denote the frequency band and the pair of D/A channels used. Two dashed lines are plotted with the slope corresponding to P^+/P^- of white noise and WMAP7 data, respectively.

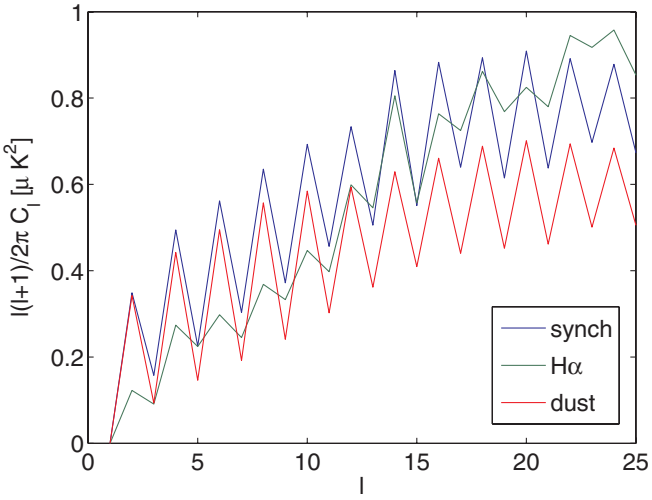

FIG. 9 (color online). The power spectra of the templates (synchrotron, Hα, dust), plotted with arbitrary normalization.

noise maps of WMAP7 data by subtracting one D/A map from other D/A data of the same frequency channel. In Fig. 8, we show P^+ and P^- values of the noise maps. As shown in Fig. 8, the noise maps do not show odd-parity preference, but their P^+/P^- ratios are consistent with that of white noise (i.e., $C_l = \text{const}$). Besides that, the signal-to-noise ratio of WMAP temperature data is quite high at low multipoles (e.g., $\text{S/N} \sim 100$ for $l = 30$) [36,43,51]. Therefore, we find that instrument noise, including $1/f$ noise, is unlikely to be the cause of the odd-parity preference.

C. Foreground

There is contamination from galactic and extragalactic foregrounds. In order to reduce foreground contamination, the WMAP team has subtracted diffuse foregrounds by template-fitting, and masked the regions that cannot be cleaned reliably. For foreground templates (dust, free-free emission, and synchrotron), the WMAP team used the dust emission model 8 Hα map, and the difference between K and Ka band maps [3,52–55]. In Fig. 9, we show the power spectrum of templates. As shown in Fig. 9, templates show strong even-parity preference, which is opposite to that of the WMAP power spectrum data. Therefore, one might attribute the odd-parity preference of WMAP data to over-subtraction by the templates. However, we find the error associated with template-fitting is unlikely to be the cause of the odd-parity preference. Consider spherical harmonic coefficients of a foreground-reduced map:

$$a_{\text{lm}}^{\text{obs}} = a_{\text{lm}}^{\text{cmb}} + a_{\text{lm}}^{\text{fg}} - b a_{\text{lm}}^{\text{tpl}}, \tag{8}$$

where $a_{\text{lm}}^{\text{obs}}$, $a_{\text{lm}}^{\text{fg}}$, and $b a_{\text{lm}}^{\text{tpl}}$ correspond to a foreground-cleaned map, a foreground, and a template with a fitting coefficient b. For simplicity, we consider only a single foreground component, but the conclusion is equally valid for multicomponent foregrounds. Because there is no correlation between foregrounds and CMB, the observed power spectrum is given by

$$C_l^{\text{obs}} \approx C_l^{\text{cmb}} + \langle |a_{\text{lm}}^{\text{fg}} - b a_{\text{lm}}^{\text{tpl}}|^2 \rangle. \tag{9}$$

As shown in Eq. (9), the parity preference should follow that of templates because of the second term, provided templates are good tracers of foregrounds (i.e., $a_{\text{lm}}^{\text{fg}}/a_{\text{lm}}^{\text{tpl}} \approx \text{const}$). Nevertheless, Eq. (9) may make a bad approximation for lowest multipoles, because the cross term $\sum_m \text{Re}[a_{\text{lm}}^{\text{cmb}}(a_{\text{lm}}^{\text{fg}} - b a_{\text{lm}}^{\text{tpl}})^*]$ may not be negligible. Besides that, our argument and the template-fitting method itself fail if templates are not good tracers of foregrounds. In order to investigate these issues, we have resorted to simulation in combination with the WMAP data. Noting the WMAP power spectrum is estimated from foreground-reduced V and W band maps, we have produced simulated maps as follows:

$$T(\hat{\mathbf{n}}) = T_{\text{cmb}}(\hat{\mathbf{n}}) + (V(\hat{\mathbf{n}}) - W(\hat{\mathbf{n}}))/2, \tag{10}$$

where $V(\hat{\mathbf{n}})$ and $W(\hat{\mathbf{n}})$ are foreground-reduced V and W band maps of WMAP data. Note that the second term on the right-hand side contains only residual foregrounds at the V and W bands, because the difference of distinct frequency channels is mainly residual foregrounds at low l. Just as with the cut-sky simulation described in Sec. II, we have applied a foreground mask to the simulated maps, and estimated the power spectrum from cut-sky by a pixel-based maximum likelihood method. In Fig. 10, we show

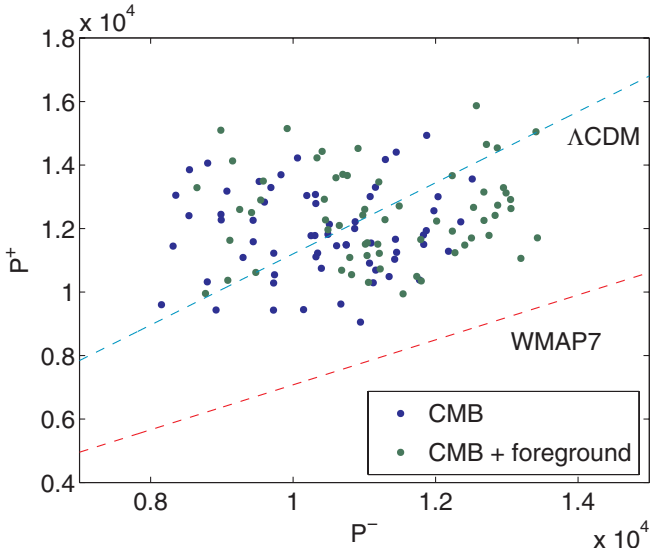

FIG. 10 (color online). Parity asymmetry in the presence of residual foregrounds (V-W): Dashed lines are plotted with slopes corresponding to P^+/P^- of P^+/P^- of ΛCDM (cyan) and WMAP7 data (red).

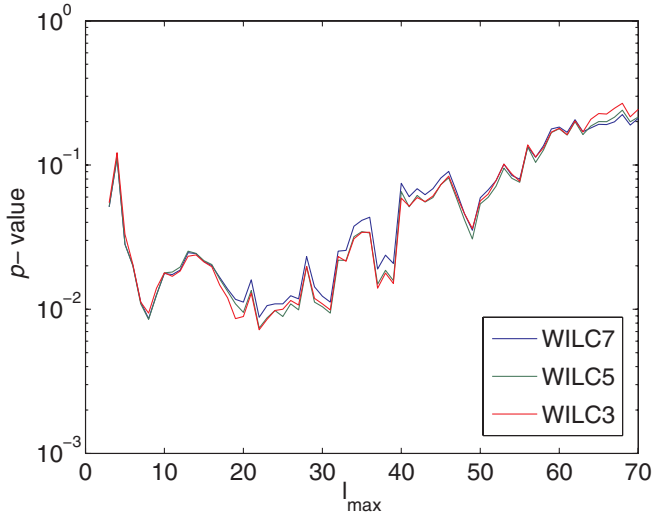

FIG. 11 (color online). Probability of getting P^+/P^- as low as the ILC 7-year, 5-year, and 3-year map at multipole range $2 \leq l \leq l_{\max}$.

P^+ and P^- values estimated from simulations. For comparison, we have included simulations without residual foregrounds, and dashed lines of a slope corresponding to P^+/P^- of the ΛCDM model and WMAP7 data. As shown in Fig. 10, the P^+/P^- of simulations in the presence of residual foregrounds does not show anomalous odd-parity preference of WMAP data. Considering Eq. (9) and simulations, we find it difficult to attribute the odd-parity preference to residual foreground.

There also exists contamination from unresolved extragalactic point sources [36]. However, point sources follow Poisson distribution with little departure [56], and therefore are unlikely to possess odd-parity preference. Besides that, point sources at WMAP frequencies are subdominant on large angular scales (low l) [36,52,56,57].

Though we have not found an association of foregrounds with the anomaly, we do not rule out residual foreground completely, because of our limited knowledge on residual foregrounds.

D. Cut sky

The WMAP team have masked the region that cannot be reliably cleaned by template fitting, and estimated CMB power spectrum from sky data outside the mask [1,4,36,52]. Therefore, we have estimated the p-value presented in Sec. II, by comparing WMAP data with cut-sky simulations. Nonetheless, we have investigated the WMAP team's internal linear combination map (ILC) map in order to see if the odd-parity preference also exists in a whole-sky CMB map. Note that the WMAP ILC map provides a reliable estimate of the CMB signal over the whole sky on angular scales larger than 10° [36,52,57]. We have compared P^+/P^- of the ILC maps with whole-sky simulations. In Fig. 11, we show p-values of the ILC maps, respectively, for various $l_{\max}$. As shown in Fig. 11, the odd-parity preference of ILC maps is most anomalous for $l_{\max} = 22$ as well. In Table III, we summarize P^+/P^- and p-values for $l_{\max} = 22$.

TABLE III. The parity asymmetry of WMAP ILC maps ($2 \leq l \leq 22$).

Data	P^+/P^-	p-value
ILC7	0.7726	0.0088
ILC5	0.7673	0.0074
ILC3	0.7662	0.0072

As shown in Fig. 11 and Table III, we find anomalous odd-parity preference exists in whole-sky CMB maps as well. Therefore, we find it difficult to attribute the anomaly to a cut-sky effect.

E. Other known sources of errors

Besides contamination discussed in previous sections, there are other sources of contamination such as sidelobe pickup and so on. In order to investigate these effects, we have resorted to simulation produced by the WMAP team. According to the WMAP team, time-ordered data (TOD) have been simulated with realistic noise, thermal drifts in instrument gains and baselines, smearing of the sky signal due to finite integration time, transmission imbalance, and far-sidelobe beam pickup. Using the same data pipeline used for real data, the WMAP team has processed simu-

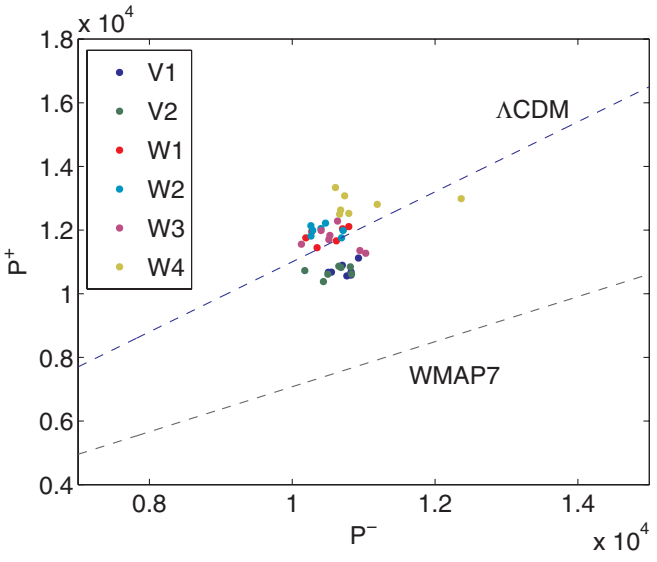

FIG. 12 (color online). P^+ and P^- of the WMAP team's simulation for V and W band data.

lated TOD, and produced maps for each differencing assembly and each single-year observation. In Fig. 12, we show the P^+ and P^- of the simulated maps, where the power spectrum estimation is made from the cut-sky by a pixel-based likelihood method. As shown in Fig. 12, all points are well above P^+/P^- of WMAP7, and agree with the ΛCDM model. Therefore, we do not find definite association of the parity asymmetry with known systematics effects.

V. COSMOLOGICAL ORIGIN

In this section, we are going to take the WMAP power spectrum at face value, and consider cosmological origins. Topological models including the multiconnected universe and Bianchi VII models have been proposed to explain the cold spot or low quadrupole power [58–60]. However, the topological models do not produce the parity asymmetry, though some of them, indeed, predict low quadrupole power. Trans-Planckian effects and some inflation models predict oscillatory features in the primordial power spectrum [61–72]. However, oscillatory or sharp features in the primordial power spectrum are smeared out in translation to the CMB power spectrum [73]. Besides, reconstruction of the primordial power spectrum and investigation on features show that the primordial power spectrum is close to a featureless power-law spectrum [1,37,38,72,74–76]. Therefore, we find it difficult to attribute the anomaly to a trans-Planckian effect or extended inflation models. We will consider what the odd-parity preference implies on primordial perturbation $\Phi(\mathbf{k})$, if the primordial power spectrum is indeed featureless. Using Eq. (A2), we may show that the decomposition coefficients of CMB anisotropy are given by

$$\begin{aligned} a_{\mathrm{lm}} &= \frac{(-\imath)^l}{2\pi^2}\int_0^\infty dk\int_0^\pi d\theta_{\mathbf{k}}\sin\theta_{\mathbf{k}}\int_0^{2\pi} d\phi_{\mathbf{k}}\Phi(\mathbf{k})g_l(k) \\ &\quad\times Y^*_{\mathrm{lm}}(\hat{\mathbf{k}}), \\ &= \frac{(-\imath)^l}{2\pi^2}\int_0^\infty dk\int_0^\pi d\theta_{\mathbf{k}}\sin\theta_{\mathbf{k}}\int_0^{\pi} d\phi_{\mathbf{k}} g_l(k) \\ &\quad\times (\Phi(\mathbf{k})Y^*_{\mathrm{lm}}(\hat{\mathbf{k}}) + \Phi(-\mathbf{k})Y^*_{\mathrm{lm}}(-\hat{\mathbf{k}})), \\ &= \frac{(-\imath)^l}{2\pi^2}\int_0^\infty dk\int_0^\pi d\theta_{\mathbf{k}}\sin\theta_{\mathbf{k}}\int_0^{\pi} d\phi_{\mathbf{k}} g_l(k)Y^*_{\mathrm{lm}}(\hat{\mathbf{k}}) \\ &\quad\times (\Phi(\mathbf{k}) + (-1)^l\Phi^*(\mathbf{k})), \end{aligned}$$

where we used the reality condition $\Phi(-\mathbf{k}) = \Phi^*(\mathbf{k})$ and $Y_{\mathrm{lm}}(-\hat{\mathbf{n}}) = (-1)^l Y_{\mathrm{lm}}(\hat{\mathbf{n}})$. Using Eq. (11), it is trivial to show, for the odd-number multipoles $l = 2n - 1$,

$$\begin{aligned} a_{\mathrm{lm}} &= -\frac{(-\imath)^{l-1}}{\pi^2}\int_0^\infty dk\int_0^\pi d\theta_{\mathbf{k}}\sin\theta_{\mathbf{k}}\int_0^{\pi} d\phi_{\mathbf{k}} g_l(k) \\ &\quad\times Y^*_{\mathrm{lm}}(\hat{\mathbf{k}})\mathrm{Im}[\Phi(\mathbf{k})], \end{aligned} \tag{11}$$

and, for even number multipoles $l = 2n$,

$$\begin{aligned} a_{\mathrm{lm}} &= \frac{(-\imath)^{l}}{\pi^2}\int_0^\infty dk\int_0^\pi d\theta_{\mathbf{k}}\sin\theta_{\mathbf{k}}\int_0^{\pi} d\phi_{\mathbf{k}} g_l(k)Y^*_{\mathrm{lm}}(\hat{\mathbf{k}}) \\ &\quad\times \mathrm{Re}[\Phi(\mathbf{k})]. \end{aligned} \tag{12}$$

It should be noted that the above equations are simple reformulations of Eq. (A2), and exactly equal to them.

From Eqs. (11) and (12), we may see that the odd-parity preference might be produced, provided

$$|\mathrm{Re}[\Phi(\mathbf{k})]| \ll |\mathrm{Im}[\Phi(\mathbf{k})]| (k \lesssim 22/\eta_0), \tag{13}$$

where η_0 is the present conformal time. Taking into account the reality condition $\Phi(-\mathbf{k}) = \Phi^*(\mathbf{k})$, we may show that primordial perturbation in real space is given by

$$\begin{aligned} \Phi(\mathbf{x}) &= 2\int_0^\infty dk\int_0^\pi d\theta_{\mathbf{k}}\sin\theta_{\mathbf{k}}\int_0^{\pi} d\phi_{\mathbf{k}} \times (\mathrm{Re}[\Phi(\mathbf{k})] \\ &\quad\times\cos(\mathbf{k}\cdot\mathbf{x}) - \mathrm{Im}[\Phi(\mathbf{k})]\sin(\mathbf{k}\cdot\mathbf{x})). \end{aligned} \tag{14}$$

Noting Eqs. (13) and (14), we find our primordial Universe may possess odd-parity preference on large scales ($2/\eta_0 \lesssim k \lesssim 22/\eta_0$). The odd-parity preference of our primordial Universe violates large-scale translational invariance in all directions. However, it is not in direct conflict with the current data on the observable Universe (i.e., WMAP CMB data), though it may seem intriguing. Considering Eqs. (13) and (14), we find this effect will be manifested on scales larger than $2\pi\eta_0/22 \approx 4$ Gpc. However, it will be difficult to observe such large-scale effects in non-CMB observations. If the odd-parity preference is indeed cosmological, it indicates we are at a special place in the Universe, which may sound bizarre. However, it should be noted that the invalidity of the Copernican principle, such as our living near the center of a void, has been previously proposed in different context [77,78].

Depending on the type of cosmological origins [e.g., topology, features in primordial power spectrum and Eq. (13)], distinct anomalies are predicted in the polarization power spectrum. Therefore, polarization maps of large-sky coverage (i.e., low multipoles) will allow us to remove degeneracy and figure a cosmological origin, if the parity asymmetry is indeed cosmological.

VI. DISCUSSION

We have investigated the parity asymmetry of our early Universe, using the newly released WMAP 7-year power spectrum data. Our investigation shows anomalous odd-parity preference of the WMAP7 data ($2 \leq l \leq 22$) at a 3-in-1000 level. When we account for our posteriori choice on $l_{\max}$, the statistical significance decreases to a 2-in-100 level, but remains significant.

There exist several known CMB anomalies at low multipole, including the parity asymmetry discussed in this paper [16–23,33,79] (see [34] for a review). We find it likely that there exists a common underlying origin, whether cosmological or not.

We have investigated noncosmological origins, and ruled out various noncosmological origins such as asymmetric beams, noise, and the cut-sky effect. We have also investigated the WMAP team's simulation, which includes all known systematic effects, and we do not find definite association with known systematics. Among cosmological origins, topological models or the primordial power spectrum of some features might provide theoretical explanation, though currently available models do not. We also find that primordial origin requires $|\mathrm{Re}[\Phi(\mathbf{k})]| \ll |\mathrm{Im}[\Phi(\mathbf{k})]|$ for $k \lesssim 22/\eta_0$, if we consider a simple phenomenologically fitting model. In other words, it requires violation of translation invariance in the primordial Universe on scales larger than 4 Gpc.

Depending on the type of cosmological origins, distinct anomalies are predicted in the polarization power spectrum. Therefore, we will be able to remove degeneracy in cosmological origins, when polarization data of large-sky coverage are available. However, at this moment, it is not even clear whether the anomaly is due to unaccounted contamination or indeed cosmological. Nonetheless, we may be able to resolve the mystery of the large-scale odd-parity preference, when data from the Planck surveyor are available.

ACKNOWLEDGMENTS

We are grateful to the anonymous referee for thorough reading and helpful comments, which led to significant improvement of this work. We thank Eiichiro Komatsu, Paolo Natoli, and Dominik Schwarz for useful discussion. We acknowledge the use of the Legacy Archive for Microwave Background Data Analysis (LAMBDA). We acknowledge the use of the simulated CMB maps of asymmetric beams produced by Wehus *et al.* [49]. Our data analysis made the use of HEALPIX [81,82]. This work is supported in part by Danmarks Grundforskningsfond, which allowed the establishment of the Danish Discovery Center. This work is supported by FNU Grant Nos. 272-06-0417, 272-07-0528, and 21-04-0355.

APPENDIX A: STATISTICAL PROPERTIES OF CMB ANISOTROPY

The CMB temperature anisotropy over a whole sky is conveniently decomposed in terms of spherical harmonics $Y_{\mathrm{lm}}(\theta, \phi)$ as follows:

$$T(\hat{\mathbf{n}}) = \sum_{\mathrm{lm}} a_{\mathrm{lm}} Y_{\mathrm{lm}}(\hat{\mathbf{n}}), \tag{A1}$$

where a_{lm} is a decomposition coefficient and $\hat{\mathbf{n}}$ is a sky direction. Decomposition coefficients are related to primordial perturbation as follows:

$$a_{\mathrm{lm}} = 4\pi(-\imath)^l \int \frac{d^3\mathbf{k}}{(2\pi)^3} \Phi(\mathbf{k}) g_l(k) Y^*_{\mathrm{lm}}(\hat{\mathbf{k}}), \tag{A2}$$

where $\Phi(\mathbf{k})$ is primordial perturbation in Fourier space and $g_l(k)$ is a radiation transfer function. For a Gaussian model for primordial perturbation, decomposition coefficients satisfy the following statistical properties:

$$\langle a_{\mathrm{lm}} \rangle = 0, \tag{A3}$$

$$\langle a^*_{\mathrm{lm}} a_{l'm'} \rangle = C_l \delta_{\mathrm{ll}'} \delta_{\mathrm{mm}'}, \tag{A4}$$

where $\langle \ldots \rangle$ denotes the average over the ensemble of universes. Given a standard cosmological model, a Sachs-Wolf plateau is expected at low multipoles [80]: $l(l+1)C_l \sim$ const.

[1] D. Larson, J. Dunkley, G. Hinshaw, E. Komatsu, M. R. Nolta, C. L. Bennett, B. Gold, M. Halpern, R. S. Hill, N. Jarosik, A. Kogut, M. Limon, S. S. Meyer, N. Odegard, L. Page, K. M. Smith, D. N. Spergel, G. S. Tucker, J. L. Weiland, E. Wollack, and E. L. Wright, arXiv:1001.4635.

[2] N. Jarosik, C. L. Bennett, J. Dunkley, B. Gold, M. R. Greason, M. Halpern, R. S. Hill, G. Hinshaw, A. Kogut, E. Komatsu, D. Larson, M. Limon, S. S. Meyer, M. R. Nolta, N. Odegard, L. Page, K. M. Smith, D. N. Spergel, G. S. Tucker, J. L. Weiland, E. Wollack, and E. L. Wright,

arXiv:1001.4744.
[3] G. Hinshaw *et al.*, Astrophys. J. **180**, 225 (2009).
[4] M. R. Nolta *et al.*, Astrophys. J. Suppl. Ser. **180**, 296 (2009).
[5] J. Dunkley *et al.*, Astrophys. J. **180**, 306 (2009).
[6] M. C. Runyan *et al.*, Astrophys. J. **149**, 265 (2003).
[7] C. L. Reichardt *et al.*, Astrophys. J. **694**, 1200 (2009).
[8] P. Ade *et al.*, Astrophys. J. **674**, 22 (2008).
[9] C. Pryke *et al.*, Astrophys. J. **692**, 1247 (2009).
[10] J. Hinderks *et al.* Astrophys. J. **692**, 1221 (2009).
[11] G. Efstathiou, C. Lawrence, J. Tauber *et al.* (Planck Collaboration), arXiv:astro-ph/0604069.
[12] M. Cruz, E. Martínez-González, P. Vielva, and L. Cayón, Mon. Not. R. Astron. Soc. **356**, 29 (2005).
[13] M. Cruz, M. Tucci, E. Martínez-González, and P. Vielva, Mon. Not. R. Astron. Soc. **369**, 57 (2006).
[14] M. Cruz, L. Cayón, E. Martínez-González, P. Vielva, and J. Jin, Astrophys. J. **655**, 11 (2007).
[15] M. Cruz, E. Martínez-González, P. Vielva, J. M. Diego, M. Hobson, and N. Turok, Mon. Not. R. Astron. Soc. **390**, 913 (2008).
[16] Angélica de Oliveira-Costa, Max Tegmark, Matias Zaldarriaga, and Andrew Hamilton, Phys. Rev. D **69**, 063516 (2004).
[17] C. J. Copi, D. Huterer, and G. D. Starkman, Phys. Rev. D **70**, 043515 (2004).
[18] D. J. Schwarz, G. D. Starkman, D. Huterer, and C. J. Copi, Phys. Rev. Lett. **93**, 221301 (2004).
[19] C. J. Copi, D. Huterer, D. J. Schwarz, and G. D. Starkman, Mon. Not. R. Astron. Soc. **367**, 79 (2006).
[20] C. J. Copi, D. Huterer, D. J. Schwarz, and G. D. Starkman, Phys. Rev. D **75**, 023507 (2007).
[21] K. Land and J. Magueijo, Phys. Rev. Lett. **95**, 071301 (2005).
[22] K. Land and J. Magueijo, Mon. Not. R. Astron. Soc. **378**, 153 (2007).
[23] A. Rakić and D. J. Schwarz, Phys. Rev. D **75**, 103002 (2007).
[24] K. Land and J. Magueijo, Phys. Rev. D **72**, 101302 (2005).
[25] C.-G. Park, Mon. Not. R. Astron. Soc. **349**, 313 (2004).
[26] L.-Y. Chiang, P. D. Naselsky, O. V. Verkhodanov, and M. J. Way, Astrophys. J. Lett. **590**, L65 (2003).
[27] Pavel D. Naselsky, Lung-Yih Chiang, Poul Olesen, and Oleg V. Verkhodanov, Astrophys. J. **615**, 45 (2004).
[28] H. K. Eriksen, F. K. Hansen, A. J. Banday, K. M. Górski, and P. B. Lilje, Astrophys. J. **609**, 1198 (2004).
[29] F. K. Hansen, A. J. Banday, K. M. Gorski, H. K. Eriksen, and P. B. Lilje, Astrophys. J. **704**, 1448 (2009).
[30] J. Hoftuft, H. K. Eriksen, A. J. Banday, K. M. Gorski, F. K. Hansen, and P. B. Lilje, Astrophys. J. **699**, 985 (2009).
[31] J. Kim and P. Naselsky, J. Cosmol. Astropart. Phys. 7 (2009) 041.
[32] J. Kim and P. Naselsky, Phys. Rev. D **79**, 123006 (2009).
[33] J. Kim and P. Naselsky, Astrophys. J. Lett. **714**, L265 (2010).
[34] C. J. Copi, D. Huterer, D. J. Schwarz, and G. D. Starkman, arXiv:1004.5602.
[35] George B. Arfken and Hans J. Weber, *Mathematical Methods for Physicists* (Academic, New York, 2000), 5th ed.
[36] G. Hinshaw *et al.*, Astrophys. J. **170**, 288 (2007).
[37] E. Komatsu *et al.*, Astrophys. J. **180**, 330 (2009).
[38] E. Komatsu, K. M. Smith, J. Dunkley, C. L. Bennett, B. Gold, G. Hinshaw, N. Jarosik, D. Larson, M. R. Nolta, L. Page, D. N. Spergel, M. Halpern, R. S. Hill, A. Kogut, M. Limon, S. S. Meyer, N. Odegard, G. S. Tucker, J. L. Weiland, E. Wollack, and E. L. Wright, arXiv:1001.4538.
[39] J. R. Bond, A. H. Jaffe, and L. Knox, Phys. Rev. D **57**, 2117 (1998).
[40] G. Efstathiou, Mon. Not. R. Astron. Soc. **370**, 343 (2006).
[41] B. D. Wandelt, E. Hivon, and K. M. Górski Phys. Rev. D **64**, 083003 (2001).
[42] E. Hivon, K. M. Górski, C. B. Netterfield, B. P. Crill, S. Prunet, and F. Hansen Astrophys. J. **567**, 2 (2002).
[43] R. S. Hill *et al.*, Astrophys. J. **180**, 246 (2009).
[44] H. K. Eriksen, I. J. O'Dwyer, J. B. Jewell, B. D. Wandelt, D. L. Larson, K. M. Górski, S. Levin, A. J. Banday, and P. B. Lilje, Astrophys. J. **155**, 227 (2004).
[45] Antony Lewis and Sarah Bridle, computer code COSMOMC ++, ver. 8, 2006.
[46] Antony Lewis and Sarah Bridle, Phys. Rev. D **66**, 103511 (2002).
[47] Harold Jeffreys, *Theory of Probability* (Oxford University, New York, 1998), 3rd ed.
[48] N. Jarosik, C. Barnes, M. R. Greason, R. S. Hill, M. R. Nolta, N. Odegard, J. L. Weiland, R. Bean, C. L. Bennett, O. Doré, M. Halpern, G. Hinshaw, A. Kogut, E. Komatsu, M. Limon, S. S. Meyer, L. Page, D. N. Spergel, G. S. Tucker, E. Wollack, and E. L. Wright, Astrophys. J. **170**, 263 (2007).
[49] I. Kathrine Wehus, L. Ackerman, H. K. Eriksen, and N. E. Groeneboom, Astrophys. J. **707**, 343 (2009).
[50] George Rieke, *Detection of Light: From the Ultraviolet to Submillimeter* (Cambridge University Press, Cambridge, England, 2002), 2nd ed.
[51] G. Hinshaw, C. Barnes, C. L. Bennett, M. R. Greason, M. Halpern, R. S. Hill, N. Jarosik, A. Kogut, M. Limon, S. S. Meyer, N. Odegard, L. Page, D. N. Spergel, G. S. Tucker, J. L. Weiland, E. Wollack, and E. L. Wright, Astrophys. J. **148**, 63 (2003).
[52] B. Gold, N. Odegard, J. L. Weiland, R. S. Hill, A. Kogut, C. L. Bennett, G. Hinshaw, J. Dunkley, M. Halpern, N. Jarosik, E. Komatsu, D. Larson, M. Limon, S. S. Meyer, M. R. Nolta, L. Page, K. M. Smith, D. N. Spergel, G. S. Tucker, E. Wollack, and E. L. Wright arXiv:1001.4555.
[53] Douglas P. Finkbeiner, Marc Davis, and David J. Schlegel, Astrophys. J. **524**, 867 (1999).
[54] D. P. Finkbeiner, Astrophys. J. **146**, 407 (2003).
[55] C. L. Bennett, R. S. Hill, G. Hinshaw, M. R. Nolta, N. Odegard, L. Page, D. N. Spergel, J. L. Weiland, E. L. Wright, M. Halpern, N. Jarosik, A. Kogut, M. Limon, S. S. Meyer, G. S. Tucker, and E. Wollack, Astrophys. J. **148**, 97 (2003).
[56] M. Tegmark and G. Efstathiou, Mon. Not. R. Astron. Soc. **281**, 1297 (1996).
[57] B. Gold *et al.*, Astrophys. J. **180**, 265 (2009).
[58] G. Efstathiou, Mon. Not. R. Astron. Soc. **346**, L26 (2003).
[59] A. Niarchou and A. Jaffe Phys. Rev. Lett. **99**, 081302 (2007).
[60] K. Land and J. Magueijo, Mon. Not. R. Astron. Soc. **367**, 1714 (2006).

[61] Andrew R. Liddle and David H. Lyth, *Cosmological Inflation and Large-Scale Structure* (Cambridge University Press, Cambridge, England, 2000), 1st ed.
[62] J. Martin and R. H. Brandenberger, Phys. Rev. D **63**, 123501 (2001).
[63] J. Martin and R. Brandenberger, Phys. Rev. D **68**, 063513 (2003).
[64] U. H. Danielsson, Phys. Rev. D **66**, 023511 (2002).
[65] R. Easther, B. R. Greene, W. H. Kinney, and G. Shiu, Phys. Rev. D **66**, 023518 (2002).
[66] N. Kaloper, M. Kleban, A. Lawrence, and S. Shenker, Phys. Rev. D **66**, 123510 (2002).
[67] J. Martin and C. Ringeval, Phys. Rev. D **69**, 083515 (2004).
[68] C. P. Burgess, J. M. Cline, F. Lemieux, and R. Holman, J. High Energy Phys. 2 (2003) 048.
[69] K. Schalm, G. Shiu, and J. P. van der Schaar, J. High Energy Phys. 4 (2004) 076.
[70] R. Easther, W. H. Kinney, and H. Peiris, J. Cosmol. Astropart. Phys. 8 (2005) 001.
[71] R. Easther, W. H. Kinney, and H. Peiris, J. Cosmol. Astropart. Phys. 5 (2005) 009.
[72] D. N. Spergel *et al.*, Astrophys. J. **170**, 377 (2007).
[73] C. L. Bennett, R. S. Hill, G. Hinshaw, D. Larson, K. M. Smith, J. Dunkley, B. Gold, M. Halpern, N. Jarosik, A. Kogut, E. Komatsu, M. Limon, S. S. Meyer, M. R. Nolta, N. Odegard, L. Page, D. N. Spergel, G. S. Tucker, J. L. Weiland, E. Wollack, and E. L. Wright, arXiv:1001.4758.
[74] S. L. Bridle, A. M. Lewis, J. Weller, and G. Efstathiou, Mon. Not. R. Astron. Soc. **342**, L72 (2003).
[75] G. Nicholson, C. R. Contaldi, and P. Paykari, J. Cosmol. Astropart. Phys. 1 (2010) 016.
[76] J. Hamann, A. Shafieloo, and T. Souradeep, J. Cosmol. Astropart. Phys. 4 (2010) 010.
[77] S. Alexander, T. Biswas, A. Notari, and D. Vaid, J. Cosmol. Astropart. Phys. 9 (2009) 025.
[78] T. Clifton, P. G. Ferreira, and K. Land, Phys. Rev. Lett. **101**, 131302 (2008).
[79] C. J. Copi, D. Huterer, D. J. Schwarz, and G. D. Starkman, Mon. Not. R. Astron. Soc. **399**, 295 (2009).
[80] Scott Dodelson, *Modern Cosmology* (Academic, New York, 2003), 2nd ed.
[81] K. M. Gorski, B. D. Wandelt, F. K. Hansen, E. Hivon, and A. J. Banday, Astrophys. J. **622**, 759 (2005).
[82] K. M. Gorski, E. Hivon, A. J. Banday, B. D. Wandelt, F. K. Hansen, M. Reinecke, and M. Bartelman, Astrophys. J. **622**, 759 (2005).